Postprint

This is the accepted version of a paper published in *Chemistry of Materials*. This paper has been peer-reviewed but does not include the final publisher proof-corrections or journal pagination.

Access to the published version may require subscription.

N.B. When citing this work, cite the original published paper.

# Ion Trapping and De-trapping in Amorphous Tungsten Oxide Thin Films Observed by Real-time Electro-optical Monitoring

Rui-Tao Wen,[a,*] Miguel A. Arvizu,[a] Michael Morales-Luna,[a] Claes G. Granqvist[a] and Gunnar A. Niklasson[a]

[a]Department of Engineering Sciences, The Ångström Laboratory, Uppsala University, P. O. Box 534, SE-75121 Uppsala, Sweden

## ABSTRACT

Several technologies for energy saving and storage rely on ion exchange between electrodes and electrolytes. In amorphous electrode materials, detailed knowledge of Li-ion intercalation is hampered by limited information on the structure and transport properties of the materials. Amorphous tungsten oxide is the most studied electrochromic material and suffers from ion-trapping-induced degradation of charge capacity and optical modulation span upon extensive electrochemical cycling. In this paper, we investigate trapping and de-trapping processes in connection with performance degradation and specifically use real-time electro-optical monitoring to identify different trap energy ranges pertinent to the ion-intercalated system. Evidence is presented for three kinds of traps which degrade electrochromic tungsten oxide during ion intercalation: (*i*) shallow traps which erode the colored state, (*ii*) deep traps which lower the bleached-state transmittance, and (*iii*) irreversible traps. Importantly, Li-ion de-trapping from shallow and deep traps takes place by different processes: continuous Li-ion extraction is possible from shallow traps, whereas a certain release time must be exceeded for de-trapping from deep traps. Our notions for ion trapping and de-trapping, presented here, may serve as a starting point for discussing ion intercalation in various amorphous materials of interest for energy-related applications.

## INTRODUCTION

Intercalation and de-intercalation of lithium ions in amorphous oxides has been extensively studied because of the manifold applications of these materials in energy-storage and energy-saving devices such as rechargeable lithium-ion batteries[1-4] and electrochromic (EC) windows.[5-8] In EC devices, optically transparent $WO_3$ can switch reversibly between dark blue and transparent states under the action of a small potential which induces ion insertion or extraction.[7,9] This property renders thin films of $WO_3$ of keen interest for "smart windows", which have a great potential for controlling solar heat gain and daylighting in energy-efficient buildings.[10-12] Coloration takes place upon Li-ion intercalation into the $WO_3$ structure along with insertion of charge-compensating electrons from the outer circuit, thereby shifting the position of the Fermi level into the conduction band in the electronic density of states of $WO_3$,[13,14] whereas bleaching is due to the return of the Fermi level to the band gap by electron extraction. Ideally, this Fermi level shift is completely reversible so that the EC device can operate indefinitely without performance degradation. However, inability to extract all of the intercalated ions during a single electrochemical cycle leads to pronounced ion accumulation in the host after many cycles[15,16] thus degrading electrochemical reversibility and optical modulation span.[9, 17-21]

Recent work of ours associated this degradation with ion trapping.[9,16] The underlying trapping mechanism is still far from clear, and it was proposed in earlier work by Bisquert[22,23] that the host structure has two kinds of intercalation sites referred to by him as "fast" diffusion sites and "slow" trap sites (this notation will be modified below) where the latter were able to immobilize diffusing ions. We found that ions in trap sites could be liberated by running a weak constant current through a bleached $WO_3$ film and again immobilized upon a second filling with ions.[9,18] Hence ion-trapping-induced EC degradation can be effectively eliminated

through a galvanostatic de-trapping process and, importantly from a practical perspective, degraded $WO_3$ films can be rejuvenated and regain their EC performance.[18]

Unlike the case of crystalline materials whose accessible intercalation sites are known for a given crystal structure,[7,24,25] amorphous materials exhibit complex intercalation processes associated with structural disorder and in amorphous $WO_3$, which is the topic of our present work, this disorder prevails throughout the intercalation process. The amorphous structures may contain dangling bonds[26] as well as irregular atomic coordination polyhedra. The intercalation in amorphous $WO_3$ involves a very wide energy distribution,[27] rather than distinct intercalation energies as in the crystalline structure, where these energies are associated with phase transitions.[24] Hence amorphous structures and trapping of intercalated ions make it natural to consider energetic inhomogeneity of the host matrix.[22, 27, 28]

In this paper, we explore the energetic disorder in $WO_3$ with regard to various traps in the intercalated material by *in situ* electro-optical monitoring. We find three main types of traps in amorphous EC $WO_3$: (*i*) *shallow traps* which only degrade the colored state, (*ii*) *deep traps* which significantly degrade the bleached state, and (*iii*) *irreversible traps* for permanently immobilized ions. Furthermore we propose interpretations for our experimental observations. Importantly, we identify shallow and deep traps by a *potentiostatic* de-trapping technique rather than galvanostatically as before.[6,12,14] (We note that the nomenclature in this paper is somewhat different from the one in earlier work of ours[9] in order to permit a more elaborate description of the observed phenomena.)

## EXPERIMENTAL SECTION

Reactive direct current magnetron sputtering was used to deposit $WO_3$ thin films in a coating system based on a Balzers UTT 400 unit. Glass plates were pre-coated with $In_2O_3$:Sn (ITO, 60 $\Omega$ per square) and used as substrates. The target was a 5-cm-diameter plate of metallic

tungsten with a purity of 99.95%. The sputtering chamber was first pumped to ~6×10⁻⁵ Pa, and pre-sputtering took place in an atmosphere of argon (99.998%) and oxygen (99.998%) for a few minutes to ensure purity of the subsequently prepared samples. Film uniformity was accomplished by substrate rotation, and no heating was used during the whole deposition process. The $O_2$/Ar gas-flow ratio and the sputtering power were set at constant values of 13% and 200 W, respectively, and the pressure in the chamber was maintained at ~4 Pa during thin film deposition in order to create a porous structure. The $WO_3$ films were found to be x-ray amorphous. Their thicknesses were 300 ± 10 nm as determined by surface profilometry using a DektakXT instrument.

Electrochemical measurements were conducted by use of a Solartron 1286 Electrochemical Interface. Cyclic voltammetry, as well as potentiostatic and galvanostatic de-trapping, were performed in a three-electrode electrochemical cell. The electrochemical and *in situ* optical measurements were performed in an argon-filled glove box whose water content was below ~0.5 ppm. The working electrode was the $WO_3$ film, which was immersed in an electrolyte of 1M $LiClO_4$ dissolved in propylene carbonate. The counter and reference electrodes consisted of Li foils. Potentiostatic and galvanostatic techniques were used to extract the trapped Li ions from degraded $WO_3$ films; specifically, a constant potential in the range 4.5–5.75 V or a constant current density of ~3.0 $\mu$A cm⁻², was applied in the direction opposite to the one yielding Li ion insertion in the $WO_3$. Charge capacity $C$ was obtained from CV data according to $C = \int \frac{jdV}{s}$, where $j$ is current density, $s$ is scan rate and $V$ is voltage. The open circuit potential, i.e. the potential of the working electrode under open circuit conditions, was measured before and after each experiment.

*In situ* optical transmittance was measured in the range of visible light (400–800 nm wavelength interval) during the electrochemical operations by the use of a fiber-optical instrument from Ocean Optics. The electrochemical cell was positioned between a tungsten

halogen lamp and the detector, and the 100-%-level was taken as the transmittance recorded before immersion of the sample in the electrolyte.

## RESULTS AND DISCUSSION

The voltammetric experiment commenced with a commonly used potential range for amorphous $WO_3$, *viz.*, 2.0–4.0 V, which leads to the simplest situation. The starting point for the cyclic voltammograms was at the open-circuit potential (OCP, ~3.5 V), and 500 CV cycles were performed, which continuously lowered the charge capacity and OCP (~2.9 V after 500 cycles) by ion trapping[9] as illustrated in Figure 1a and 1b. Optical transmittance modulation decreased concomitantly and solely by degradation of the colored state whereas the bleached state remained unchanged (Figure 1c). As mentioned above, the larger optical absorption in the colored state ensues from the Fermi level moving into the conduction band of $WO_3$.[13,14] Ion trapping make the reversible intercalation sites fewer and fewer and block sites that would otherwise be effective for EC absorption; the corresponding trapping sites are referred to as "shallow". The change in the OCP of ~0.6 eV is consistent with a shift of the conduction band by the same amount towards higher energy, since the film is still transparent in the bleached state.
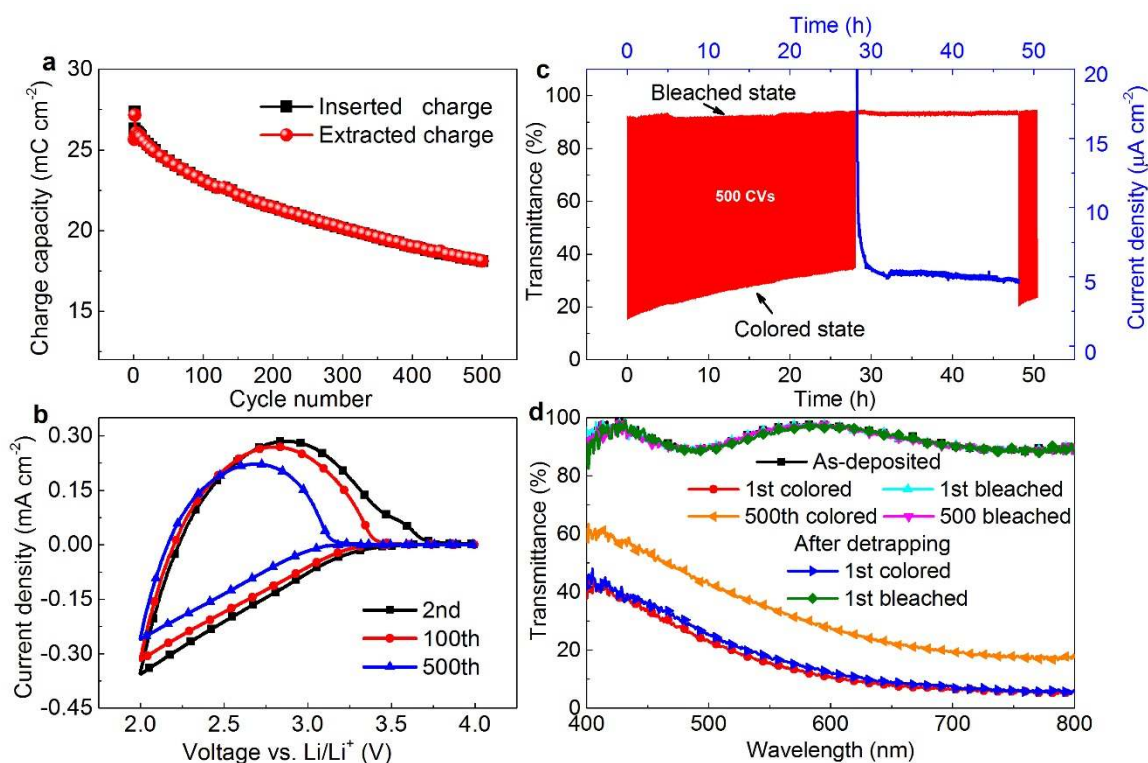
**Figure 1**. Electrochemical and electrochromic performance of a ~300-nm-thick amorphous WO$_3$ film studied in the range of 2.0–4.0 V *vs*. Li/Li$^+$. (a) Charge capacity evolution upon ion intercalation and de-intercalation during cyclic voltammetry (CV) for 500 cycles. (b) CV data, at the shown cycle numbers, recorded with a scan rate of 20 mV s$^{-1}$. (c) *In situ* optical transmittance at a wavelength of 550 nm upon CV cycling at 20 mV s$^{-1}$, potentiostatic de-trapping at 5.5 V *vs*. Li/Li$^+$ for 20 h, and finally CV cycling under the same conditions; blue (L-shaped) curve shows current density evolution during de-trapping. (d) *In situ* spectral optical transmittance in the 400–800-nm wavelength interval for the as-deposited state, after the indicated number of CV cycles, and subsequent to de-trapping (optical transmittance data for as-deposited and bleached states overlap).

In our previous study,[9] degraded WO$_3$ thin films were rejuvenated by galvanostatic de-trapping. The potential then increased to ~5.5 V during the first few minutes, and it remained at this value until the end of the experiment after 20 h. Here, we instead apply a *constant potential* of 5.5 V for 20 h to refresh the degraded WO$_3$ film. As indicated by the blue (L-shaped) curve in Figure 1c, the current density drops very rapidly and then attains an almost constant value for the rest of the potentiostatic experiment. Integrating the current, we obtain a charge density of ~11 mC cm$^{-2}$ after subtraction of a constant background, clearly observed

at long times, which we associate with parasitic electrochemical processes such as electrolyte degradation.[9,29] This charge density is of the same order of magnitude as the difference in charge capacity between the first and 500th CV cycle in Figure 1a. As for galvanostatic de-trapping,[9] the optical transmittance was unaltered during the whole de-trapping process whereas the OCP increased from ~2.9 to ~3.5 V. CV cycling was conducted after the potentiostatic de-trapping and showed that the initial EC performance was regained (Figure 1c). The overlapping spectral transmittance data (Figure 1d) for films in as-deposited and de-trapped conditions confirm the elimination of the ion-trapping-induced EC degradation. Efficient Li-ion intercalation can be achieved when the scan rate is very low, *i.e.*, 0.1 mV s$^{-1}$. Clearly the intercalation of Li ions into amorphous $WO_3$ takes places over a broad potential range (*i.e.*, large energy distribution), and the absence of distinct features indicates solid-solution behavior between $WO_3$ and $Li_xWO_3$ (Figure S1), which is similar to Li-ion intercalation into amorphous $TiO_2$.[2] As shown by x-ray diffraction applied to the film reported on in Figure S1, any structural rearrangements during the intercalation process must take place within the amorphous state (Figure S2).

Figure 2 presents further data on charge capacity and optical transmittance under various electrochemical operations on a $WO_3$ film. This film was first severely degraded as above and was then subjected to potentiostatic de-trapping at 5.5 V during shorter time periods than before—specifically for 1, 2, and 4 h—which made the current density decrease as shown in Figure S3. Charge capacity evolution was investigated by recording 10 CV cycles after each of the de-trapping procedures (Figure 2a). The gradual recovery of the charge capacity and optical modulation span after each potentiostatic de-trapping period demonstrates that Li-ion de-trapping from shallow traps is a continuous process (and qualitatively different from the situation for deep traps, as shown next).
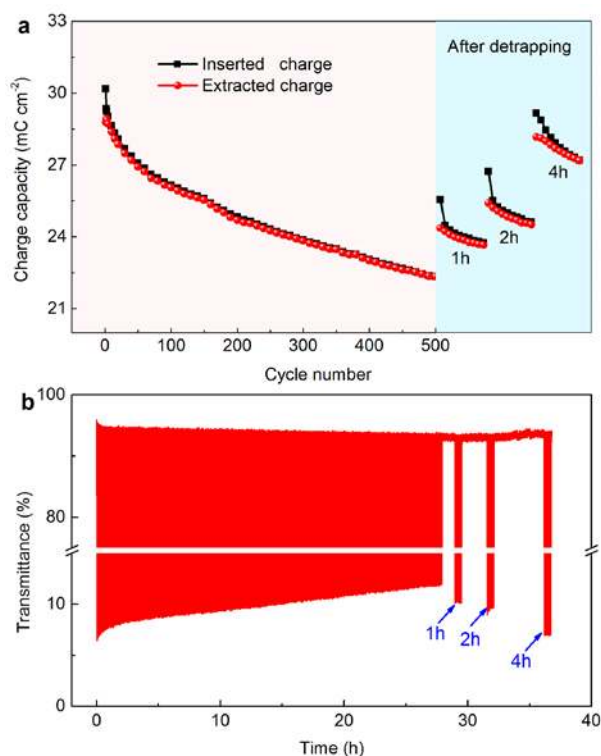
**Figure 2**. Electrochemical and electrochromic performance of a ~300-nm-thick amorphous $WO_3$ film studied in the range of 2.0–4.0 V *vs*. Li/Li$^+$ at a scan rate of 20 mV s$^{-1}$. (a) Charge capacity evolution upon 500 cyclic voltammetry (CV) cycles followed by potentiostatic ion de-trapping at 5.5 V *vs*. Li/Li$^+$ for the stated durations, with interspersed CV cycling (10 cycles). (b) Corresponding *in situ* optical transmittance at a wavelength of 550 nm (the transmittance scales differ for the high- and low-transmittance ranges).

Studies of $WO_3$ films were conducted also in the wider potential range of 1.5–4.0 V and demonstrated new and striking features that were not present for the previous range of 2.0–4.0 V. Prior to electrochemical cycling in the wide potential range, we ran 10 CV cycles at 2.0–4.0 V and 20 mV s$^{-1}$ to establish a baseline and allow easy comparison with earlier data. Then 20 CV cycles were run at 1.5–4.0 V and 10 mV s$^{-1}$, which led to severe shrinking of the encircled areas in the CV data in Figure 3a; the corresponding decrease of the OCP was from ~3.5 to ~2.0 V. Large unbalances were noted for inserted and extracted charge densities during the initial ~10 CV cycles whereas approximate equality between inserted and extracted charge capacity prevailed for cycle numbers 10–20 (Figure 3b). By summing up the unbalance between inserted and extracted charge, the amount of trapped charge was found to

correspond to ~70 mC cm$^{-2}$. Our observations may indicate that the trap sites are almost fully occupied after a small number of CV cycles or, alternatively, that increased trapping in the host structure leads to electrostatic repulsion between Li ions becoming stronger and preventing subsequent trapping.

Figure 3c shows *in situ* optical transmittance under varied electrochemical operations and presents evidence for severe degradation of a WO$_3$ film upon 20 CV cycles in the range of 1.5–4.0 V. Clearly, not only the colored state but also the bleached state is now affected, which differs from the observations for the 2.0–4.0 V range for which only the colored state was influenced. Evidently more energy is required to affect the bleached state than the colored state. We use the term "deep" traps to denote the sites for the Li ions responsible for degrading the bleached state.

To test whether the severely degraded WO$_3$ film can be refreshed by potentiostatic de-trapping, a constant potential of 5.5 V was applied during a 20-h period after the electrochemical cycling, as elaborated in Figure 3c. The optical transmittance increased somewhat at the inception of the de-trapping process, and the transmittance then maintained approximately the same value until a conspicuous abrupt increase to the initial optical transmittance took place after ~2.5 h and signaled successful de-trapping of Li ions from deep traps. Current density evolution during potentiostatic de-trapping is presented by the blue curve in Figure 3c, which demonstrates that a distinct peak in the current density concurs with the sharp onset of high optical transmittance. It therefore appears that an energy barrier has to be overcome in order to liberate the ions from the deep traps; this is distinctly different from the case of the shallow traps discussed above.

After completion of the de-trapping process, the initial optical transmittance was recovered except for a minor difference at short wavelengths (Figure 3d, black and orange curves at

400–500 nm). The slight residual absorption emanates from what we refer to as "irreversible" traps from which the Li ions cannot be retrieved under the present experimental conditions. Hence the de-trapped WO₃ film possessed essentially the same EC performance as in its initial state, as corroborated by a final round of 10 CV cycles in the range of 2.0–4.0 V and comparison with the first 10 CV cycles recorded under the same conditions (Figure 3c).
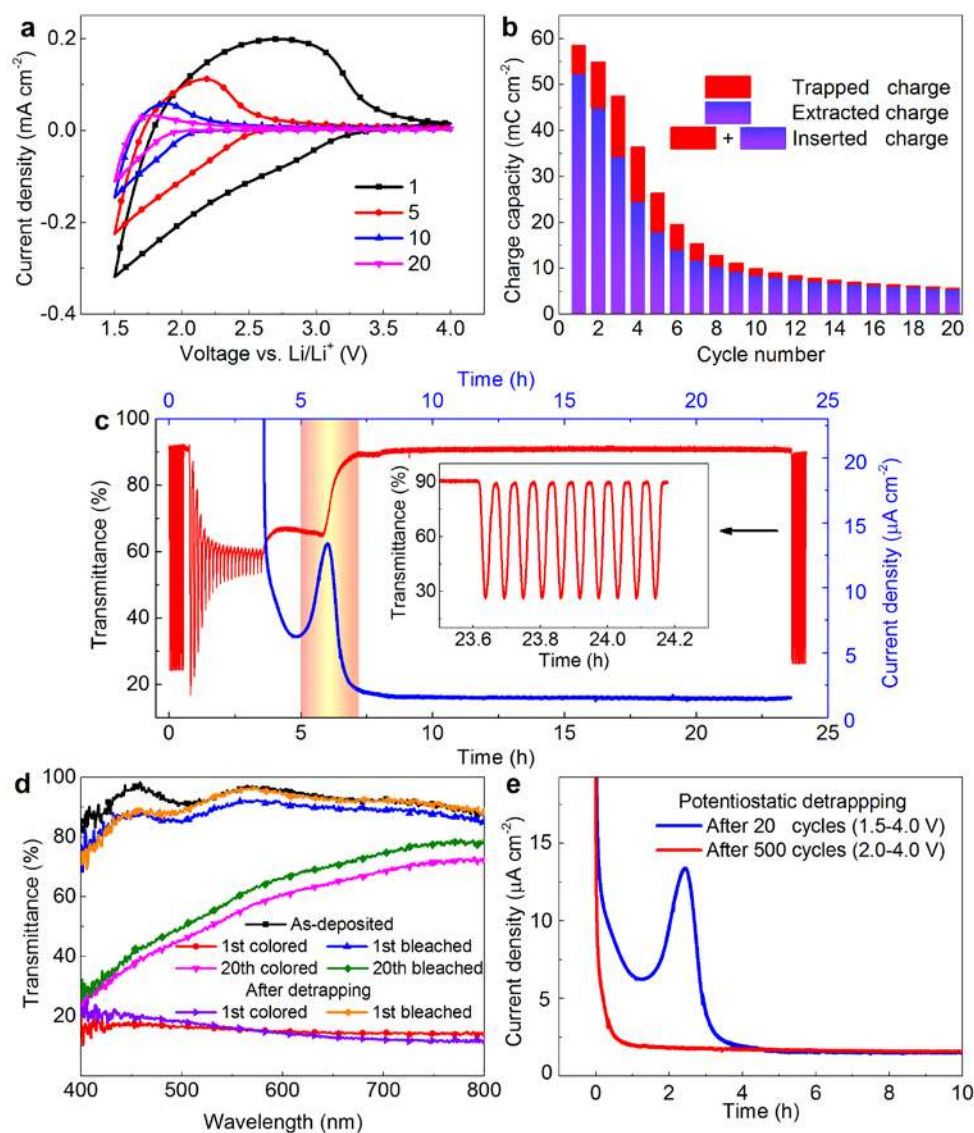


**Figure 3**. Electrochemical and electrochromic performance of ~300-nm-thick amorphous WO₃ films. (a) Cyclic voltammetry (CV) data, at the shown cycle numbers, recorded in the range of 1.5–4.0 V *vs.* Li/Li⁺ at a scan rate of 10 mV s⁻¹. (b) Charge capacity for ion intercalation and de-intercalation during 20 CV cycles run as in (a). (c) *In situ* optical transmittance at a wavelength of 550 nm upon varied electrochemical treatments, and current density (with a peak after ~6 h) under potentiostatic de-trapping; the electrochemical operations were as follows: (*i*) 10 CV cycles were run in the range of

2.0–4.0 V *vs.* Li/Li$^+$ at a scan rate of 20 mV s$^{-1}$ followed by a resting period of 10 minutes, (*ii*) 20 CV cycles were then run in the range of 1.5–4.0 V *vs.* Li/Li$^+$ at a scan rate of 10 mV s$^{-1}$, (*iii*) potentiostatic ion de-trapping was subsequently performed for 20 h at a potential of 5.5 V *vs.* Li/Li$^+$, and finally (*iv*) 10 CV cycles were run as in (*i*) (with time-resolved data displayed in the inset). (d) *In situ* spectral optical transmittance in the 400–800-nm wavelength range after CV cycling in the range of 1.5–4.0 V *vs.* Li/Li$^+$ at a scan rate of 10 mV s$^{-1}$; data are shown for the as-deposited state, after the indicated number of CV cycles, and subsequent to de-trapping (optical transmittance data for the as-deposited and bleached states overlap partly). (e) Current density evolution during potentiostatic de-trapping for the shown potential ranges and numbers of cycles.

Figure 3e gives a detailed comparison of the current density evolution during potentiostatic de-trapping of WO$_3$ films cycled in the two potential ranges; the effect of de-trapping from deep traps can be clearly distinguished as a peak whereas de-trapping from shallow traps proceeds as a continuous process. The integrated current corresponds to a charge density of ~72 mC cm$^{-2}$ after subtraction of a constant background due to electrolyte degradation.[9,29] This charge release agrees well with the charge that was trapped during the initial 20 CV cycles.

Some complementary studies on the effects of ion trapping and de-trapping were performed galvanostatically and are presented in Figure S4, where we show the EC performance of a WO$_3$ film prior to the abrupt onset of optical transmittance. As before, we ran 10 CV cycles with 2.0–4.0 V and 20 mV s$^{-1}$ followed by 20 CV cycles with 1.5–4.0 V and 10 mV s$^{-1}$ to degrade the film's properties, and galvanostatic de-trapping at a current density of ~3.0 $\mu$A cm$^{-2}$ was then carried out during 2 h. The optical transmittance increased only slightly during this de-trapping process, possibly as a result of ion removal from shallow traps, but there was no sharp increase of optical transmittance. 10 CV cycles with 2.0–4.0 V and 20 mV s$^{-1}$ were subsequently run so that the charge capacity and optical modulation could be compared with those of the initial state. It was observed that the film was almost unable to sustain Li-ion intercalation and optical modulation. However a subsequent complete galvanostatic de-

trapping procedure, conducted during 20 h, led to an abrupt onset of high optical transmittance as before (see also data in earlier work of ours[9]).

Data until now have reported de-trapping at a constant potential $U_D$ equal to 5.5 V, but we also investigated the effect of having other voltages in order to provide more insights into the details of the de-trapping of Li ions in $WO_3$ that had undergone degradation at 1.5–4.0 V following procedures described above (see caption of Figure 3). As shown from the evolution of current density (Figure 4a) and optical transmittance (Figure 4b), we were unable to remove ions from deep traps for $U_D \leq 5.0$ V. Above this de-trapping voltage, however, the current density evolution became qualitatively different and displayed peaks that became increasingly narrow and took place after shorter and shorter times when $U_D$ was increased. These peaks concurred with the abrupt increases in bleached state transmittance as seen in Figure 4b.

The appearance of distinct peaks in the current density indicates that the kinetics of the process is limited by removal of ions from deep traps. Assuming a thermally activated process, the release frequency $f_p \approx 1/t_p$ can be written as

$$f_p = v_0 exp(-E_a/k_B T),  \tag{1}$$

where $t_p$ is the time from the beginning of the de-trapping experiment to the occurrence of the peak, $v_0$ is taken to be a characteristic Li–O vibrational frequency ($\sim 8 \times 10^{13}$ s$^{-1}$),[30] $E_a$ is activation energy, $k_B$ is Boltzmann's constant, and $T$ is temperature. Empirical $t_p$ values of ~1–6 h correspond to activation energies of ~1.0–1.05 eV.
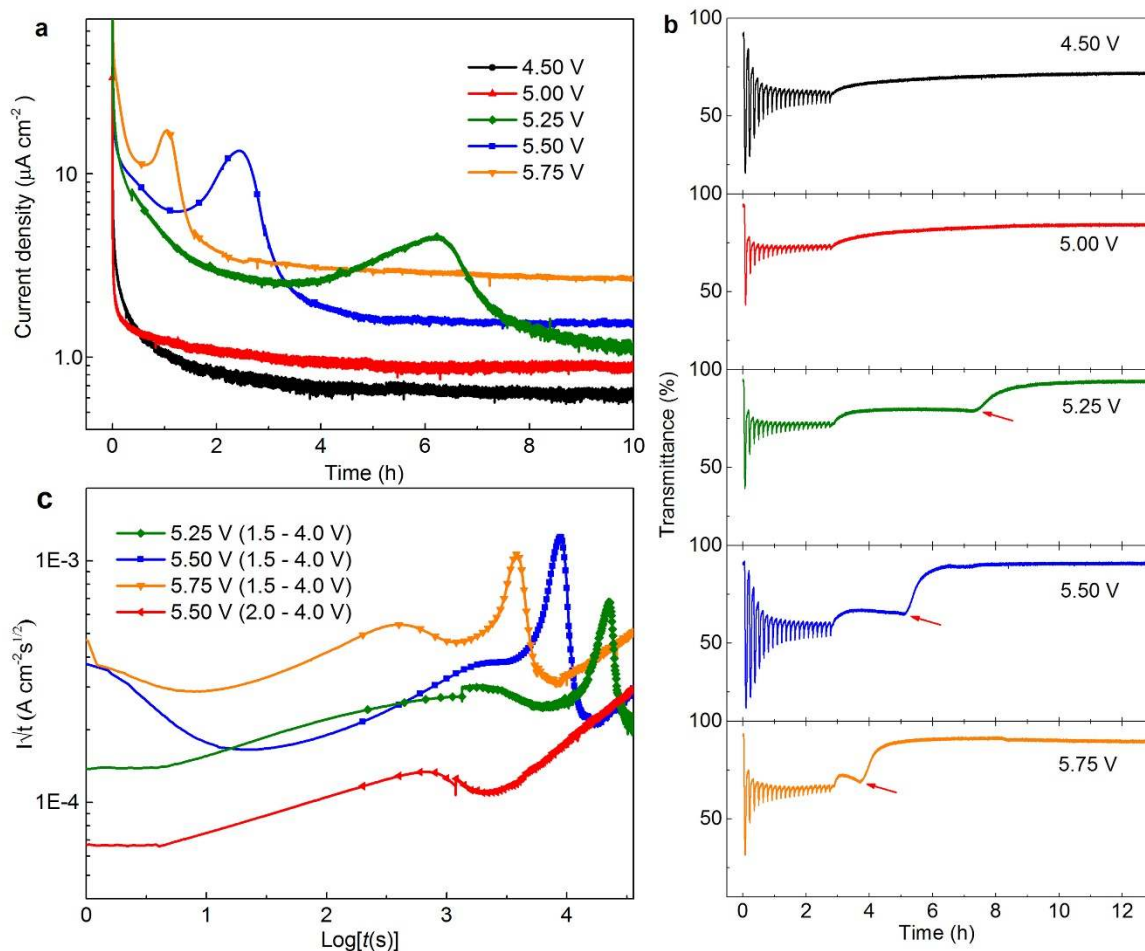
**Figure 4.** Current density and electrochromic performance for ~300-nm-thick amorphous $WO_3$ films, degraded as described in the caption of Figure 3, subjected to potentiostatic de-trapping at the shown potentials ($U_D$). (a) Current density evolution and (b) corresponding *in situ* optical transmittance at a wavelength of 550 nm (arrows indicate the onset of de-trapping); data for $U_D$ = 5.5 V were shown also in Figure 3. (c) Cottrell plot showing current density (*I*) multiplied by the square root of time ($t^{1/2}$, with *t* in seconds) *vs*. log(*t*); a supplementary plot is shown for degradation at 2.0–4.0 V *vs*. Li/Li$^+$ and de-trapping at $U_D$ = 5.5 V (the minor irregularities at log(*t*) ≈ 3 are experimental artifacts).

The current peaks are superimposed on a continuously decreasing background similar to the one observed for samples degraded by CV cycling between 2 and 4 V (Figure 1c), and we argued above that this component is due to release of ions from shallow traps. This situation can be analyzed as outlined by Montella,[31] who has made a detailed theoretical study of

current transients governed by combined effects of diffusion and reaction kinetics. Figure 4c shows a so called Cottrell plot of current density $I$ times $t^{1/2}$ as a function of $\log(t)$, where $t$ is time,[32] which displays significant departures from a pure diffusion-limited behavior (which would have yielded a horizontal line). Specifically, a secondary peak appears at a time that is much shorter than that for the main current peak discussed above. The sample degraded at 2–4 V also shows a very similar feature in Figure 4c. Montella[31] demonstrated that it is possible to determine an effective diffusion coefficient $D_{eff}$ from the (short-time) peak value in the Cottrell plot via

$$D_{eff} = \pi L^2 \left( I(t)\sqrt{t} \right)_p^2 / (\Delta Q)^2 , \qquad (2)$$

where $L$ is film thickness, $\Delta Q$ is charge passed during the process after subtraction of the charge responsible for electrolyte degradation, and subscript $p$ denotes the peak value for $\left( I(t)\sqrt{t} \right)$. We find $D_{eff}$ to be of the order of $10^{-17}$–$10^{-16}$ m$^2$ s$^{-1}$, which is consistent with previous measurements of the diffusion coefficient of Li$^+$ in WO$_3$ [33] and considering that the effective value obtained from Eq. 2 can be a severe underestimation.[31]

**CONCLUSIONS**

In summary, although intercalation and de-intercalation processes are complex in amorphous systems, it was possible to extract significant and detailed information for electrochromic amorphous WO$_3$ thin films through judiciously designed experiments. By combining electrochemical experiments with *in situ* optical monitoring we identified—in addition to the reversible diffusion sites—three different types of Li-ion traps which we denote "shallow", "deep" and "irreversible". Furthermore, we demonstrated that heavily degraded WO$_3$ films could be rejuvenated by potentiostatic de-trapping of Li ions. The de-trapping processes were found to be different for shallow and deep traps: continuous Li-ion extraction took place from shallow traps whereas de-trapping from deep traps occurred by excitation over an energy

barrier. Trapping in shallow states does not affect the bleached-state transmittance in electrochromic $WO_3$, and the rejuvenation current is controlled by the kinetics of both diffusion and trapping. On the other hand, trapping in deep traps leads to large optical absorption also for the bleached state and the rejuvenation process is controlled by release of ions from traps with activation energy of ~1 eV. The chemical reactions underlying the various trapping and rejuvenation mechanisms are not known in detail, but it has been demonstrated that Li compounds, for example $Li_2O$, can form at low potentials either inside $WO_3$ or as a solid–electrolyte interface.[25,34,35] We finally note that ion-trapping is a ubiquitous phenomenon in ion-intercalated materials, and the present findings may have implications also for degradation and performance recuperation of rechargeable batteries and other ion-exchange-based devices.

## ASSOCIATED CONTENT

**Supporting Information.** Data are given on (*i*) cyclic voltammetry at a very slow scan rate of 0.1 mV s$^{-1}$, (*ii*) X-ray diffractometry on as-deposited, colored, bleached and de-trapped films, (*iii*) current density *vs*. time during potentiostatic de-trapping for different periods of time, and (*iv*) charge capacity and *in situ* optical transmittance after various electrochemical operations, including galvanostratic de-trapping. All data were recorded on ~300-nm-thick $WO_3$ films.

## AUTHOR INFORMATION
### Corresponding Author
*Rui-Tao Wen, E-mail: Ruitaow@mit.edu.

Present Address: Materials Processing Center, Massachusetts Institute of Technology, Cambridge, Massachusetts 02139, United States.

### Notes
The authors declare no competing financial interest.

# REFERENCES

(1)  Whittingham, M. S. Ultimate Limits to Intercalation Reactions for Lithium Batteries. *Chem. Rev.* **2014**, 114, 11414.

(2) Borghols, W. J. H.; Lützenkirchen-Hecht, D.; Haake, U.; Chan, W.; Lafont, U.; Kelder, E. M.; van Eck, E. R. H.; Kentgens, A.P.; Mulder, F. M.; Wagemaker. M. Lithium Storage in Amorphous $TiO_2$ Nanoparticles. *J. Electrochem. Soc.* **2010**, 157, A582.

(3) Berg, H. Batteries for Electric Vehicles: Materials and Electrochemistry. Cambridge University Press, Cambridge, UK, 2015.

(4) Zheng, Y.; Ouyang, M.; Lu, L.; Li, J. Understanding Ageing Mechanisms in Lithium-ion Battery Packs: From Cell Capacity Loss to Pack Quality Evolution. *J. Power Sources* **2015**, 278, 278.

(5) Granqvist, C. G. Electrochromic Materials: Out of a Niche. *Nat. Mater.* **2006**, 5, 89.

(6) Llordes, A.; Garcia, G.; Gazquez, J.;  Milliron, D. J. Tunable Near-infrared and Visible Light Transmittance in Nanocrystal-in-glass Composites. *Nature* **2013**, 500, 323.

(7) Granqvist, C. G. Handbook of Inorganic Electrochromic Materials. Elsevier, Amsterdam, The Netherlands, 1995.

(8) Mortimer, R. J.; Rosseinsky, D. R.; Monk, P. M. S.; editors, Electrochromic Materials and Devices, Wiley-VCH, Weinheim, Germany. 2015.

(9) Wen, R.-T.; Granqvist, C. G.; Niklasson, G. A. Eliminating Degradation and Uncovering Ion-trapping Dynamics in Electrochromic $WO_3$ Thin Films. *Nat. Mater.* **2015**, 14, 996.

(10) Smith, G. B.; Granqvist, C. G.; Green Nanotechnology: Solutions for Sustainability and Energy in the Built Environment. CRC Press, Boca Raton, FL, USA, 2010.

(11) Jelle, B. P. Solar Radiation Glazing Factors for Window Panes, Glass Structures and Electrochromic Windows in Buildings—Measurement and Calculation. *Sol. Energ. Mater. Sol. Cells* **2013**,116, 291.

(12) Granqvist, C. G. Electrochromics for Smart Windows: Oxide-based Thin Films and Devices. *Thin Solid Films* **2014**, 564, 1.

(13) Niklasson, G. A.; Granqvist, C. G.; Electrochromics for Smart Windows: Thin Films of Tungsten Oxide and Nickel Oxide, and Devices Based on These. *J. Mater. Chem.* **2007**, 17, 127.

(14) Goodenough, J. B. in Progress in Solid State Chemistry, ed. H. Reiss (Pergamon, Oxford, UK, 1971), vol. 5, p. 145.

(15) Bueno, P. R.; Faria, R. C.; Avellaneda, C. O.; Leite, E. R.; Bulhões, L. O. S. $Li^+$ Insertion into Pure and Doped Amorphous $WO_3$ Films. Correlations between Coloration Kinetics, Charge and Mass Accumulation. *Solid State Ionics* **2003**,158, 415.

(16) Arvizu, M.; Wen, R.-T.; Primetzhofer, D.; Klemberg-Sapieha, J.; Martinu, L.; Niklasson, G. A.; Granqvist, C.G. Galvanostatic Ion De-trapping Rejuvenates Oxide Thin Films. *ACS Appl. Mater. Interfaces* **2015**, 7, 26387.

(17) Kim, J.; Ong, G. K.; Wang, Y.; LeBlanc, G.; Williams, T. E.; Mattox, T. M.; Helms, B. A.; Milliron, D. J. Nanocomposite Architecture for Rapid, Spectrally-Selective Electrochromic Modulation of Solar Transmittance. *Nano Lett.* **2015**, 15, 5574.

(18) Wen, R.-T.; Niklasson, G. A.; Granqvist, C. G. Sustainable Rejuvenation of Electrochromic $WO_3$ Films. *ACS Appl. Mater. Interfaces* **2015**, 7, 28100.

(19) Yoo, S. J.; Lim, J. W.; Choi, B.; Sung, Y.-E. Enhanced Reliability of Electrochromic Devices with a LiPON Protective Layer. *J. Electrochem. Soc.* **2007**, 154, P6.

(20) Lee, S.-H.; Deshpande, R.; Parilla, P. A.; Jones, K. M.; To, B.; Mahan, A. H.; Dillon, A. C. Crystalline $WO_3$ Nanoparticles for Highly Improved Electrochromic Applications. *Adv. Mater.* **2005**, 18, 763.

(21) Liu, J.-W.; Zheng, J.; Wang, J. L.; Xu, J.; Li, H. H.; Yu, S. H. Ultrathin $W_{18}O_{49}$ Nanowire Assemblies for Electrochromic Devices. *Nano Lett.* **2013**, 13, 3589.

(22) Bisquert, J. Analysis of the Kinetics of Ion Intercalation: Ion Trapping Approach to Solid-state Relaxation Processes. *Electrochim. Acta* **2002**, 47, 2435.

(23) Bisquert, J.; Vikhrenko, V. S. Analysis of the Kinetics of Ion Intercalation. Two State Model Describing the Coupling of Solid State Ion Diffusion and Ion Binding Processes. *Electrochim. Acta* **2002**, 47, 3977.

(24) Zhong, Q.; Dahn, J. R.; Colbow, K. Lithium Intercalation into $WO_3$ and the Phase Diagram of $Li_xWO_3$. *Phys. Rev. B* **1992**, 46, 2554.

(25) He, Y.; Gu, M.; Xiao, H.; Luo, L.; Shao, Y.; Gao, F.; Du, Y.; Mao, S.; Wang, C. Atomistic Conversion Reaction Mechanism of $WO_3$ in Secondary Ion Batteries of Li, Na and Ca. *Angew. Chem. Int. Ed.* **201**6, 55, 6244.

(26) Sun, C. Thermo-mechanical Behavior of Low-dimensional Systems: The Local Bond Average Approach. *Prog. Mater. Sci.* **2009**, 54, 179.

(27) Strömme, M.; Ahuja, R.; Niklasson, G. A. New Probe of the Electronic Structure of Amorphous Materials. *Phys. Rev. Lett.* **2004**, 93, 206403.

(28) Bisquert, J. Beyond the Quasistatic Approximation: Impedance and Capacitance of an Exponential Distribution of Traps. *Phys. Rev. B* **2008**, 77, 235203.

(29) Ufheil, J.; Würsig, A.; Schneider, O. D.; Novák, P. Acetone as Oxidative Decomposition Product in Propylene Carbonate Containing Battery Electrolyte. *Electrochem. Comm.* **2005**, 7, 1380.

(30) Osaka, T.; Shindo, I. Infrared Reflectivity and Raman Scattering of Lithium Oxide Single Crystals. *Solid State Commun.* **1984**, 51, 421.

(31) Montella, C. Discussion of the Potential Step Method for the Determination of the Diffusion Coefficients of Guest Species in Host Materials Part I. Influence of Charge Transfer Kinetics and Ohmic Potential Drop. *J. Electroanal. Chem.* **2002**, 518, 61.

(32) Bard, A. J.; Faulkner, L. R.; Electrochemical Methods: Fundamentals and Applications (Wiley, New York, NY, USA, 1980), p. 143.

(33) Mattsson, M. S. Li Insertion into $WO_3$: Introduction of a New Electrochemical Analysis Method and Comparison with Impedance Spectroscopy and the Galvanostatic Intermittent Titration Technique. *Solid State Ionics* **2000**, 131, 261.

(34) Bressers, P. M. M. C.; Meulenkamp, E. A. The Electrochromic Behavior of Indium Tin Oxide in Propylene Carbonate Solutions. *J. Electrochem. Soc.* **1998**, 145, 2225.

(35) Radin, M. D.;  Rodriguez, J. F.; Tian, F.; Siegel, D. J. Lithium Peroxide Surfaces Are

Metallic, While Lithium Oxide Surfaces Are Not. *J. Am. Chem. Soc.* **2011**, 134, 1093.

**Table of Contents Graphic**